Mitochondrial methionyl N-formylation affects steady-state levels of oxidative phosphorylation complexes and their organization into supercomplexes

Citation: Arguello, Tania et al. "Mitochondrial methionyl N-formylation affects steady-state levels of oxidative phosphorylation complexes and their organization into supercomplexes." Journal of Biological Chemistry 293, 39 (August 2018): 15021-15032. © 2018 Arguello et al.

As Published: http://dx.doi.org/10.1074/jbc.ra118.003838

Publisher: American Society for Biochemistry & Molecular Biology (ASBMB)

Persistent URL: https://hdl.handle.net/1721.1/125164

Version: Author's final manuscript: final author's manuscript post peer review, without publisher's formatting or copy editing

JBC Papers in Press. Published on August 7, 2018 as Manuscript RA118.003838
The latest version is at http://www.jbc.org/cgi/doi/10.1074/jbc.RA118.003838

Mitochondrial methionyl N-formylation affects oxidative phosphorylation complexes steady-state levels and their organization into supercomplexes

Tania Arguello[1], Caroline Köhrer[2,3], Uttam L. RajBhandary[2], Carlos T. Moraes[1*]

[1]Department of Neurology, University of Miami School of Medicine, Miami, Florida, USA

[2] Department of Biology, Massachusetts Institute of Technology, Cambridge, MA, USA

[3] Present address: Moderna Therapeutics, Cambridge, MA, USA.

Running title: The role of mitochondrial methionyl N-formylation

*To whom correspondence should be addressed: 1420 NW 9th Avenue, Miami, FL 33136. Phone: (305) 243-5858. cmoraes@med.miami.edu

Key words: protein synthesis, mitochondria, mitochondrial disease, methionine, gene knockout, N-formylation.

ABSTRACT

N-Formylation of the Met-tRNAMet by the nuclear-encoded mitochondrial methionyl-tRNA formyl transferase (MTFMT) has been found to be a key determinant of protein synthesis initiation in mitochondria. In humans, mutations in the MTFMT gene result in Leigh syndrome, a progressive and severe neurometabolic disorder. However, the absolute requirement of formylation of Met-tRNAMet for protein synthesis in mammalian mitochondria is still debated. Here, we generated a Mtfmt-KO mouse fibroblast cell line and demonstrated that N-formylation of the first methionine via fMet-tRNAMet by MTFMT is not an absolute requirement for initiation of protein synthesis. However, it differentially affected the efficiency of synthesis of mtDNA-coded polypeptides. Lack of methionine N-formylation did not compromise the stability of these individual subunits, but had a marked effect on the assembly and stability of the OXPHOS complexes I and IV and on their supercomplexes. In summary, N-formylation is not essential for mitochondrial protein synthesis, but is critical for efficient synthesis of several mitochondrially encoded peptides and for OXPHOS complex stability and assembly into supercomplexes

In mitochondria, synthesis of proteins requires a tightly and coordinated communication between nuclear and mitochondrial DNA. Although the majority of proteins required for the process are encoded in the nuclear DNA, translated in the cytoplasm and imported to mitochondria (1), 13 proteins which are catalytic subunits of the oxidative phosphorylation system (OXPHOS) are synthesized inside mitochondria. These proteins are encoded by the mammalian mitochondrial DNA (mtDNA) along with 22 tRNAs and 2 ribosomal rRNAs required for their synthesis.

The current model of mitochondrial protein synthesis is divided in three conserved steps as it occurs in cytoplasm: initiation, elongation and termination. In mammalian mitochondria, the initiation step acts as a major checkpoint and rate-limiting factor in protein synthesis (2). The nuclear-encoded protein methionyl-tRNA formyltransferase (MTFMT) is responsible for adding a formyl group to a portion of the single mitochondrial Met-tRNA^{Met} (3). Once the Met-tRNA is acylated/aminoacylated with methionine (Met-tRNA^{Met}) and N-formylated by MTFMT (fMet-tRNA^{Met}), it is recognized by the initiation factor mtIF2 (a translational GTPase), before it binds to the small mito-ribosomal subunit (SSU)-mRNA complex (2,3). Following this, hydrolysis of GTP into GDP facilitates the binding of the large mito-ribosomal subunit (LSU) and completes the formation of the initiation complex allowing elongation to start (4).

Although, N-formylation is considered a requirement for initiation of protein synthesis in mitochondria and most bacteria, it cannot be easily generalized across species or domains of life. For example, in different bacterial species, absence of N-formylation has been shown to strongly impair cellular growth (*E. coli*) (5), reduce viability (*S. pneumoniae*, *M. smegmatis and M. bovis)* (6) or to have only minor effects in others (*P. aeruginosa)*(7). In lower eukaryotes such as *S. cerevisiae,* N-formylation is not essential (8). In humans, different compound heterozygous mutations in MTFMT were identified in a subset of patients diagnosed with Leigh syndrome, a severe neurometabolic disorder combined with OXPHOS dysfunction (9-15), demonstrating that N-formylation is critical for OXPHOS function. Furthermore, studies in fibroblasts of patients harboring mutations in the *MTFMT* gene showed reduced activity of complex I and/or IV and in some cases complex V supporting the critical role of N-formylation for mitochondrial OXPHOS function.

MTFMT expression is required for the N-formylation of mitochondrial Met-tRNA^{Met} in patients, but there is still controversy about the absolute requirements of N-formylation for mitochondrial protein synthesis. Four compound heterozygous patients studied sharing the common c.626C>T mutation allele in the *MTFMT* gene, showed absence of MTFMT protein expression levels (9,13,14) and no detectable levels of mitochondrial fMet-tRNA^{Met} (9,13). However, all mutant fibroblasts still had mitochondrial protein synthesis, albeit at decreased efficiency.

Contradictory results were also described for the N-formylation of COI, a mitochondrially-encoded subunit of complex IV. In one study, using mutant MTFMT fibroblasts, most of the COI was not assembled into complex IV and was not N-formylated, suggesting that N-formylation of COI is required for assembly into complex IV (13). However, this finding contrasts with a previous study where, in absence of detectable levels of MTFMT expression, N-formylation of COI was still observed (9).

Biochemical studies into the common c.626C>T mutation allele mechanism argued that the c.626C>T mutation allele not only predicts to eliminate two exon splicing enhancers resulting in a truncated and not functional protein (9), but also in a missense mutation and a.S209L substitution. The authors suggested that residual activity of the S209L mutant MTFMT protein (16) could explain the observed mitochondrial protein synthesis and the detection of N-formylated-COI found in one study (9).

To clarify the function of MTFMT in mammals, we generated a complete *Mtfmt* knockout (KO) in mouse fibroblasts to determine if N-formylation on Met-tRNA^{Met} by MTFMT is an absolute requirement for

protein synthesis initiation in mammalian mitochondria. We also evaluated the effects of complete ablation of *Mtfmt* on the synthesis and stability of the 13 mitochondrially-encoded proteins, individual OXPHOS complexes and their association into supercomplexes.

RESULTS

Mtfmt homozygous knockout fibroblasts do not express MTFMT protein

In order to generate a complete *Mtfmt* KO model *ex vivo*, we deleted the exon 4 of the *Mtfmt* gene in mouse skin fibroblasts using the cre-loxP technology (17). The exon 4 flanked by LoxP sites was deleted using a plasmid expressing cre recombinase under the control of the CMV promoter. Deletion of exon 4 is predicted to result in the synthesis of a truncated protein. Exon 4 is present in all transcript isoforms and is where the most frequent disease mutation (c.626 C>T) has been found in patients with mutations in the *MTFMT* gene. After clonal selection and expansion, we confirmed the successful deletion of exon 4 by amplification of the deleted fragment by short PCR in the *Mtfmt* KO fibroblast clones and the absence of this fragment in the parental LoxP/LoxP clone (Fig. 1A). We did not detect MTFMT by western blot using enriched mitochondrial crude extracts in different *Mtfmt* KO fibroblast clones (n=3) (Fig. 1B). These observations confirmed the generation of a complete *Mtfmt* knockout model in mouse fibroblasts. KO cells grew normally in enriched high glucose media and gross mitochondrial distribution (by Mitotracker staining) also appeared similar to controls (not shown).

Mitochondrial MTFMT is responsible for N-formylation of the Met-tRNA^{Met} in mammalian mitochondria.

In mammalian mitochondria, once the unique tRNA^{Met} is acylated/aminoacylated by the methionyl-tRNA synthetase, the MTFMT adds a formyl group to a portion of Met-tRNA^{Met}. To evaluate the activity of the MTFMT, we measured the steady state-levels of the three forms of the mitochondrial tRNA^{Met}: deacylated (tRNA^{Met}), aminoacylated (Met-tRNA^{Met}) and aminoacylated and N-formylated (fMet-tRNA^{Met}). These were identified by high resolution northern blot analysis, using the cytoplasmic (Met-tRNAi^{Met}) as a negative control of N-formylation. After isolation of total RNA under acidic conditions to maintain both Met-tRNA^{Met} and fMet-tRNA^{Met}, we detected the three forms of tRNA^{Met} in the *Mtfmt* control clones (Fig. 2A) which showed lower amounts of the deacylated tRNA^{Met} form and almost equal amounts of fMet-tRNA^{Met} and Met-tRNA^{Met} (Fig. 2B). In the *Mtfmt* KO fibroblast clones instead, we did not detect fMet-tRNA^{Met} and interestingly, the KO clones showed preferential accumulation of the aminoacylated Met-tRNA^{Met} with two out of three mutant clones showing lower levels of deacylated tRNA^{Met} (Fig. 2A and 2B). We observed a marked increase of total mitochondrial tRNA^{Met} levels (Fig. 2C), similar to previous results in humans (9). These results indicate that MTFMT is required for N-formylation of the Met-tRNA^{Met} and suggest that the absence of MTFMT activity may affect the regulation of the tRNA^{Met} ratios in mammalian mitochondria.

N-formylation is not an absolute requirement for mitochondrial protein synthesis in mammalian mitochondria.

To evaluate the effects of MTFMT absence in mitochondrial protein synthesis, we measured

the metabolic incorporation of radiolabeled ^{35}S-Met-Cys in the 13 mitochondrially-encoded proteins in the presence of an irreversible inhibitor of cytoplasmic ribosomes (emetine). Using a short pulse, (15 to 30 minutes), we observed the synthesis of all 13 mitochondrially-encoded proteins in the *Mtfmt* KO cell clones relative to *Mtfmt* controls (Fig. 3A). Interestingly, the rate of synthesis varied among the individual subunits (Fig. 3C). It was drastically reduced for ND4 (83%) followed by subunits ND4L (59%), COI (57%), ND6 (56%), ND1 (53%) and COIII (47%). It was not significantly alterd for subunits CYTB (35%), COII/ATP6 (33%), ND3 (20%) and ATP8 (130%). ND5 and ND2 subunits from complex I were not detected, suggesting that both proteins have a low rate of synthesis in this fibroblast cell model, as they could be observed in pulse-chase experiments (Supplementary Fig. S2). The ND1 subunit not only showed decreased rate of synthesis in the *Mtfmt* KO clones but also faster migration relative to control cells (Fig. 3B enlarged panel). We did not detect this migration difference in two different mouse cell models of complex I deficiency (*Ndufs3* KO) and complex IV deficiency (*Cox10* KO) (Supplementary Fig. S1) which indicates that absence of N-formylation not only affects the rate of synthesis but has an additional effect on the electrophoretic mobility of this subunit. The lack of specific antibodies made it difficult to address this question as we could not to isolate ND1 to sequence the N-terminus.

Altogether these results demonstrated that in mammals, mitochondrial protein synthesis occurs in absence of N-formylation. However, lack of N-formylation compromised the efficiency of synthesis of the 13 mitochondrially-encoded polypeptides at different degree .

Absence of N-formylation does not have a marked effect in the stability of mitochondrially-encoded polypeptides.

We then wanted to investigate if absence of N-formylation has any effect on the stability of the newly synthesized mitochondrially-encoded polypeptides. For that, we determined the rate of degradation of each polypeptide in the *Mtfmt* KO cell clones relative to controls using the pulse-chase radiolabeling assay and measuring the rate of ^{35}S-Met-Cys incorporation at two different chase times (9 and 18 hours). In this assay, cells were pre-treated with chloramphenicol (a reversible mitochondrial protein synthesis inhibitor) for 24 hours, which results in the accumulation of the nuclear encoded components, required for mitochondrial protein synthesis.

Pulse-labelling with ^{35}S-Met-Cys detected all mitochondrially-encoded polypeptides, including subunits ND5 and ND2 in the *Mtfmt* KO cells, confirming the synthesis of both subunits in absence of N-formylation (Supplementary Fig. S2). After 9 hours chase, the rate of degradation as well as the turnover in *Mtfmt* control cells varied among the individual subunits. ND5 subunit was no longer detected at 9 hours, most likely due to the fast turnover rate compared with the other subunits. This was followed by subunits ND2, ND3 and ND4L which were detected at lower intensity, suggesting that the turnover of this group of proteins is quicker compared to the other remaining subunits (Supplementary Fig. S2). The rate of degradation in *Mtfmt* KO cells relative to controls was determined as the percent of decrease of ^{35}S-Met-Cys incorporated label from the pulse time point (0.5 hours) (Fig. 4). We found that while the stability of the ATP8 subunit decreased in the *Mtfmt* KO cells at 9 hour chase ($P<0.01$) and the stability of the ND4 subunit had a trend to decrease in *Mtfmt* KO cells, the remaining subunits had very similar rates of degradation. We validated these results measuring and

comparing the rate of degradation in our model to the rate of degradation in *bona fide* complex I and IV deficient cell models (Supplementary Fig. S3). We found that the stability of certain subunits was highly compromised and varied depending on the model studied (Supplementary Fig. S4 and S5), which confirms that absence of N-formylation does not have a major effect on the stability of the mitochondrially-encoded proteins.

Absence of N-formylation affects the steady-state levels of OXPHOS complexes

We tested whether the lack of MTFMT, either by reduced efficiency of synthesis of the mitochondrially-encoded subunits, or by any other mechanism, has an effect on the steady-state level of OXPHOS components. We measured the steady-state levels of different mitochondrial markers by immunoblot (Fig. 5) and found that NDUFB8, a late-stage subunit during the assembly of complex I, decreased in the *Mtfmt* KO cells ($P<0.007$), whereas NDUFA9, an early-stage assembly subunit of the hydrophilic arm of complex I, did not.

Steady-state levels of CO-IV, a nuclear-encoded subunit essential for assembly of complex IV, was markedly decreased ($P<0.006$) in the *Mtfmt* KO cells. We did not detect significant changes in the steady-state levels of COI; succinate dehydrogenase complex flavoprotein subunit A (SDHA), a catalytic subunit of complex II; ubiquinol-cytochrome c reductase core protein I (UQCRC1), a core subunit component of complex III; and ATP synthase subunit alpha (ATP5A), a subunit of complex V.

Absence of N-formylation affects preferentially complex I and IV and assembly into supercomplexes

We then analyzed the assembly of the individual OXPHOS complexes and their interactions into supercomplexes. We detected these macro-complexes using blue native polyacrylamide electrophoresis (BN-PAGE) after solubilization with digitonin. In *Mtfmt* control cells the majority of detected complex I was preferentially assembled into the respirasome structure corresponding to the CI-$CIII_2$-CIV_n form and the supercomplex CI-$CIII_2$ with a small portion still detected in the isolated CI form. In the *Mtfmt* KO clone cells instead, there was a significant decrease of total complex I (70%) with the presence of CI-$CIII_2$ but no detectable levels of CI-$CIII_2$-CIV_n or free CI (Fig. 6A and 6B), indicating that absence of N-formylation had profound consequences to complex I levels and its association into supercomplexes.

In the case of complex III, *Mtfmt* control cells showed preferential association into supercomplexes CI-$CIII_2$-CIV_n and CI-$CIII_2$ with low levels of free complex III. In the *Mtfmt* KO cells, complex III instead was lost from the CI-$CIII_2$-CIV_n, but was highly increased in the free and CI-$CIII_2$ forms. The levels of complex IV decreased by 60% in the *Mtfmt* KO cells, while total complex II levels showed a significant increase, possibly as a compensatory mechanism. Analysis of complex V did not show any change in the *Mtfmt* KO cells, however there was a slight increase in the non-membrane embedded module termed F1. Altogether, these results indicate that absence of N-formylation affects preferentially assembly of individual complex I and IV and also the supercomplex interactions, mostly in the CI-$CIII_2$-CIV_n form.

We also evaluated the activity of the individual complex I and IV and supercomplexes using the BN-PAGE in-gel activity and found a nearly identical pattern of activity to the previously observed structural changes, indicating that disruption of OXPHOS complex assembly correlates with

the observed decrease in activity in individual complex I and IV as well as the supercomplex level (Fig. 6C).

Absence of N-formylation results in increased glycolysis rate in *Mtfmt* KO cells.

In order to identify the physiologic effects of MTFMT absence in mitochondrial and cellular bioenergetics, we measured the oxygen consumption rate (OCR) and extracellular acidification rate (ECAR) in *Mtfmt* KO intact cells and compared them to controls using the XFp extracellular flux analyzer (Seahorse Biosciences).

Basal respiration was decreased by 22% in the *Mtfmt* KO cells (Fig. 7A). ATP-linked respiration did not change, nor did maximal respiratory capacity (Supplementary Fig. S6A). Consequently, spare respiratory capacity (SRC) (OCR difference between the basal and maximal respiratory capacity) increased by 59%. Although we can not explain the unalltered maximum respiration, the increase in SRC could be a consequence of alternative substrate utilization under uncoupled conditions in the KO cells.

On the other hand, basal glycolysis in the *Mtfmt* KO cells increased by 40% (P=0.0055) (Fig. 7B and Supplementary Fig. S6). Subsequent addition of oligomycin to inhibit ATP from oxidative phosphorylation, did not change the glycolytic capacity of KO cells relative to control. There was a 38% decrease in glycolytic reserve (Fig. 7B), reflecting the adaptation of KO mtfmt cells to glycolysis.

DISCUSSION

N-formylation of Met-tRNA^{Met} by the MTFMT enzyme is an exclusive mechanism of mitochondrial protein synthesis in eukaryotes. However, in mammals the absolute requirement of N-formylation to start mitochondrial protein synthesis is still debated. In this study, we generated a *Mtfmt* KO mouse fibroblast cell clone model, deleting exon 4 of the *Mtfmt* gene which in humans harbors the most frequent pathogenic allele, c.626C>T. We confirmed the complete deletion of the exon 4 at the DNA level and did not detect the MTFMT protein, demonstrating the generation of *Mtfmt* KO mouse cell lines. Because this region is required for activity (16,18), its ablation leads to the formation of a null allele, as confirmed by our findings. The availability of a complete KO allowed us to study the role of MTFMT in a well defined genetic background.

Initially, we observed that N-formylation of the mitochondrial Met-tRNA^{Met} was lacking in the *Mtfmt* KO fibroblast clones, confirming that MTFMT is required for N-formylation of the Met-tRNA^{Met} in mouse mitochondria. Our analysis of the tRNA ratios indicated that in mouse fibroblast control cells, the three forms of mitochondrial tRNA^{Met} are maintained at approximately equal ratios. Studies with human fibroblasts showed preferential accumulation of the N-formylated and deacylated forms (9). However, the significance of this variation is unknown. It is generally accepted that only a proportion of the unique Met-tRNA^{Met} inside mitochondria is N-formylated, as fMet-tRNA is needed only for initiation. However, it is not known how these ratios are regulated and how they affect mitochondrial protein synthesis. Tucker's group reasoned that in human fibroblasts, the low levels of Met-tRNA^{Met} could be a result of their rapid use during the elongation process. In mouse instead, the aminoacylated tRNA^{Met} proportion remains at levels that are similar to the other tRNA^{Met} forms. Interestingly, in mutated *MTFMT* patient cells and in the mouse *Mtfmt* KO cells, the absence of N-formylation results in a preferential accumulation of the aminoacylated tRNA^{Met} and an overall increase of total tRNA^{Met},

potentially as a compensatory mechanism. There were differences in ratios between aminoacylated and deacylated $tRNA^{Met}$ among the different *Mtfmt* KO cells, but it is not known what caused these differences.

This study also demonstrated that mitochondrial protein synthesis occurs in absence of N-formylation of the mitochondrial Met-$tRNA^{Met}$ which indicates that N-formylation of the Met-$tRNA^{Met}$ is not an absolute requirement of mitochondrial protein synthesis in mammals but instead N-formylation has a critical role in the efficiency of synthesis and possibly assembly of certain mitochondrially-encoded proteins.

It is widely accepted that mitochondria are derived from bacteria and, therefore not surprisingly, the mitochondrial translational machinery shares many features, including the N-formylation of the Met-$tRNA^{Met}$ to be used in initiation. One interesting evolutionary question is whether mitochondria continue to rely on N-formylation for protein synthesis or whether they can function without it. N-formylation of Met-$tRNA^{Met}$ was already shown to be dispensable in certain bacteria, such as *P. aeruginosa* (7), and yeast (2) providing the first clue that, at least in lower eukaryotes, formylation of the mitochondrial initiator tRNA is not an absolute requirement. In mammals, bovine mitochondrial mtIF2 initiation factor strongly prefers N-formylated fMet-$tRNA^{Met}$ over non-formylated Met-$tRNA^{Met}$ (19,20). On the other hand, bovine mtIF2 also supports protein synthesis in yeast mutants without formylated intiator tRNA (21). Our data provide evidence that the mammalian mitochondrial translational machinery can function without MTFMT, but not as efficiently.

Interestingly, in our mouse model, we found that the effect on the efficiency of synthesis is different for the various mitochondrially-encoded polypeptides. In this model, absence of N-formylation affected drastically the rate of synthesis of the ND4 subunit, less for others (ND1, ND4L, ND6, COI, COII/ATP6, COIII) and had no significant effects in the rates of CYTB, ATP8 and ND3 subunits. In humans, two other studies (13,14) have reported a preferential rate of decrease for the subunits ND1, ND5, ND4 and COII. However, it is not known if this differential susceptibility is species-specific, if it correlates with the structural properties of each subunit during assembly, or if it is connected to additional functional roles of N-terminal formylation of mitochondrially-encoded proteins, such as the generation of N-formyl peptides. In humans N-formylated hexapeptides such as ND4, ND6 and COXI are agonists of the Formyl Peptide Receptor-1 and induce chemotactic cellular responses involved in the modulation of the immune response (22,23).

We also observed a differential migration in the ND1 subunit in SDS gels. We excluded the effect of polymorphisms in this *Mtfmt* KO mouse model, which have been considered to be a major source of differences in the electrophoretic migrations observed in pulse experiments (24,25). Interestingly, by reviewing SDS gels in the literature, this differential migration pattern can also be observed in one of the patients (P1) with mutations in *MTFMT* (13). Although we attempted, efforts in sequencing the N-terminal region of ND1 were unsuccessful, mostly because there are no effective antibodies against the mouse ND1 that allowed for immunoprecipitation and MS sequencing of the N-terminus. We speculate that this change in molecular weight could reflect an alternative mechanism of synthesis in response to the absence of N-formylation such as the use of an alternative start codon for initiation or other mechanism yet to be discovered. In fact, ND1 in mouse is the only subunit that uses GUG (coding for valine) as initiator instead of a canonical codon (AUN).

Potential AUN codons do exist downstream of the regular one, which could be used instead.

The absence of N-formylation did not cause a major effect on the stability of the mitochondrial subunits in the mouse *Mtfmt* KO cells as demonstrated by the pulse-chase experiments at 9 and 18 hours. However, we showed that the absence of N-formylation did affect preferentially the steady-state levels of individual complexes I and IV and drastically impacted the organization into the CI-$CIII_2$-CIV_n supercomplex. Although this could be a simple consequence of decreased steady-state levels of mtDNA-coded subunits, it may also point to a role for N-formylation in complex assembly. The physiological role of supercomplexes is still debated, but destabilization of these supramolecular assemblies could reduce efficiency of ATP production in homeostasis or stress situations (26). The assembly of complex I was the most severely affected with approximately 70% total reduction in BN-PAGE and loss of the major supercomplex organization. Complex I has seven subunits translated in the mitochondria which are critical components of the proton translocation membrane arm. In absence of N-formylation, at least two subunits, ND4 and ND1, have shown lower levels or differential migration respectively. There was also a decrease in steady-state levels of the nuclear encoded transmembrane helix NDUFB8, which was shown to interact with ND4 subunit during complex I assembly, suggesting that N-formyl residue may have a role in the assembly process of these subunits into individual complexes which consequently may affect their interaction and stability in supercomplexes.

Absence of N-formylation did not affect the total levels of complex III in the *Mtfmt* KO cells, which correlated with the normal steady-state levels of the mitochondria UQCRC1, a core subunit of complex III and no changes in efficiency of synthesis of the only mitochondrially-encoded complex III subunit CYTB. However, there was a marked effect in the supramolecular organization of this complex. In absence of N-formylation, complex III accumulated preferentially in the free form with reduction of the CI-$CIII_2$ association and loss of the major CI-$CIII_2$-CIV_n supercomplex. Complex III has been shown to be required for stability of complex I (27) and to be preferentially organized into the CI-$CIII_2$ supercomplex under normal physiological conditions (28) which suggest that these changes in supercomplex organization could result primary from the drastic decrease of complex I.

Complex IV on the other hand showed a 60% decreased levels in absence of N-formylation which correlated with the significant decrease in efficiency of *de novo* protein synthesis of mitochondrially-encoded subunits COI and COIII and the drastic decrease in steady-state levels of the nuclear encoded COIV, an assembly factor of complex IV, indicating also an important role of N-formylation not only in the assembly/stability of this individual complex, but also the drastic effects on the major CI-$CIII_2$-CIV_n supercomplex association.

It is still unclear if N-formylation contributes to the structural stability of the supramolecular structure. Electrospray ionization mass spectrometry (ESI-MS) in bovine heart mitochondria identified that, with exception of COXIII subunit, all the 12 mitochondrial encoded proteins retain the N-formyl group (29). Studies of complex IV assembly in patient fibroblasts with mutations in the MTFMT have shown a severe decrease in N-formylated COI in the assembled complex IV, indicating that the N-formyl residue of the COI may facilitate assembly into the complex (13). However in a previous study, the levels of N-formylation of COI were detected as the most abundant form in two patient fibroblasts with mutations in the MTFMT (9). Although

it is not known what caused these contrasting differences, further studies in the mouse model should help elucidate the effects of absence of N-formylation in complex IV assembly and correlate them with the human counterpart.

Assembly/stability of individual complex V was not affected in absence of N-formylation which correlated with no changes on the steady-state levels of ATP5A, a mitochondrial membrane ATP synthase subunit alpha. The increased levels of ATP8 from complex V also showed normal rate levels which indicates that absence of N-formylation does not have a major effect on the mitochondrially–encoded subunits part of these complexes.

The functional implications of the absence of N-formylation in the *Mtfmt* KO mouse model were reflected by the reduction of activity of individual complex I and complex IV, and the levels of the major CI-$CIII_2$-CIV_n respirasome These likely explain the decrease of basal mitochondrial respiration rate and the switch to glycolysis to maintain the overall energy demand. This suggest a metabolic adaptation of the *Mtfmt* KO cells and a compromised ability to respond to stress. This is also in agreement with the lactic acidosis observed in patients with Leigh syndrome and *MTFMT* mutations and could provide insights into the clinical variability and onset of the disease (10,12).

In summary, we have generated *Mtfmt* KO fibroblast mouse cell lines and confirmed that N-formylation is not an absolute requirement for mitochondrial protein synthesis in mice, yet it is critical for efficiency of synthesis of certain mitochondrially-encoded subunits. Absence of N-formylation does not affect stability of the *de novo* synthesized subunits but instead affects drastically the assembly/stability of complexes I and IV, which has profound effects on their association into supercomplexes. The absence of N-formylation results in increased reliance on glycolysis for energy production. Although cultured fibroblasts showed normal growth and survival without MTFMT, it is possible that N-formylation is critical for optimal OXPHOS function in specific tissues or stress situations. Future experiments with animal models will help answer these questions.

EXPERIMENTAL PROCEDURES

GENERATION OF THE EX VIVO Mtfmt KNOCKOUT CELL MODEL

Dermal fibroblasts were derived from skin tissue explants from 3 month adult homozygous *Mtfmt*$^{(loxP/loxP)}$ mice followed by immortalization and transfection with the CMV cre plasmid as described elsewhere (17). Confirmation of successful recombination using cre transgene expression *ex vivo* was done by amplifying the putative deleted region in the *Mtfmt* gene after cre recombinase activity by short PCR using specific primers. DNA was extracted from the parental *Mtfmt*$^{(loxP/loxP)}$ clone and *Mtfmt* KO clone cells.

CELL CULTURE CONDITIONS

Mouse fibroblast *Mtfmt*$^{(loxP/loxP)}$ controls and *Mtfmt* KO cells were grown in T75 cm^2 cell culture flasks using DMEM high glucose, supplemented with Fetal Bovine Serum (15%; Sigma), Sodium Pyruvate (1 mM), non-essential amino acids (1X), Uridine (0.1 mg/mL), and Gentamicin (20 mg/mL) all obtained from Gibco. Cells were maintained at 37°C and 5% CO_2. *Mtfmt* control cells were used between passages 30 to 50 and *Mtfmt* KO cells between passages 20 to 30. Other controls used in these experiments, such as the mouse fibroblast cell line NIH3T3 were grown in the same cell culture conditions. All the cells used in the study were tested for mycoplasma contamination by PCR. Control (CTR) clones 1 to 3 were selected after immortalization. KO (1 to 3) clones were derived from the same parental identified as CTR 2. The same controls and knockouts are shown consistenly throughout the study.

MITOCHONDRIAL EXTRACTION

Mitochondria enriched fractions were obtained by nitrogen cavitation method with slight modifications from Gottlieb, et al (30). In brief, cells were grown to 90% confluency and collected using 0.05% trypsin-EDTA (Gibco). Pellet was washed in cavitation buffer (100 mM Sucrose, 1 mM EGTA, 20 mM MOPS pH 7.4 and 1 g/l Bovine serum albumin) (Sigma). The new pellet obtained was resuspended in cavitation buffer B (buffer A plus 10 mM Triethanolamine and 5% (w/v) Percoll (Sigma) supplemented with protein inhibitor cocktail (Roche)) and placed in the cavitation vessel. Cell disruption was achieved using nitrogen gas to 600 lb/in^2 and allowed to equilibrate for 30 minutes. Cells were collected by differential centrifugation (2500rpm and 15000rpm) to separate the crude mitochondria pellet and stored at −80°C.

MITOCHONDRIAL TRANSLATION ASSAYS

Cells were grown at 90% confluency in 6-well plates. Mitochondrial protein synthesis was performed in L-Methionine-L-Cysteine Free DMEM Media (1X), supplemented with dialyzed FBS (10%) and Sodium Pyruvate (1 mM) from Gibco. Cells were incubated for 10 minutes with Emetine (100 µg/mL) as an irreversible cytoplasmic protein inhibitor during the pulse experiments and with Anisomycin (100 µg/mL) as reversible cytoplasmic protein inhibitor during chase experiments. For the chase experiments only, cells were pre-treated with Chloramphenicol (40 µg/mL) for 24 hours. All reagents were obtained from Sigma.

Approximately 400 µCi/mL of Express [^{35}S] Methionine-Cysteine protein labeling mix (Perkin Elmer Life Sciences) were added to the media and the radioisotope labeling was performed for at least 15 to 30 minutes. This followed a short incubation of 5 minutes with DMEM media, supplemented with FBS (10%) and Sodium Pyruvate (1 mM) prior to cell collection. For the chase experiments, cells were metabolically labeled for 30 minutes (pulse) and chased at two time points (9 and 18 hours). Protein extraction was performed using RIPA buffer followed by quantification using the DC Protein Assay Kit (Bio-Rad). Approximately 40-50 µg were loaded onto SDS polyacrylamide 17.5% gel (30% acrylamide and 0.2% bis-acrylamide) (5% stacking) gel. The running buffer (1X) was adjusted to pH 8.3 before use and the gel was run at 100V for approximately 15-17 hours. Transfer was performed using nitrocellulose membranes (Bio-Rad) and the Owl™ HEP Series Semidry Electro blotting System for at least 3 hours. The membrane was dried and exposed to film for at least 4 days. Quantification of bands was done using the optiQuant software (Perkin Elmer). Fast Green FCF (0.002%) followed by scanning at 625 nm using the Odyssey Infrared Imaging System (LI–COR) or Ponceau staining were used as total protein loading controls.

SDS-POLYACRYLAMIDE GEL ELECTROPHORESIS (SDS-PAGE) AND IMMUNOBLOTTING

Steady-state protein levels were measured in mitochondria enriched fraction as described previously or in total protein homogenates. Approximately 20-40 µg of protein was mixed with Laemmli buffer (Bio-Rad) supplemented with 5% mercapthoethanol and denaturated for 15 minutes at 65°C. Samples were separated on 4-20% or 10% SDS-PAGE gels and transferred to Polyvinylidene difluoride (PVDF) membranes. Membranes were blocked with 5% milk in 0.1% Tween PBS (PBST) for 1 hour and subsequently incubated with specific primary antibodies overnight at 4°C. The antibodies used included Goat polyclonal to MTFMT (T-12) 1:500 obtained from Santa Cruz (Biotechnlogies) (sc-137618), Rabbit anti-actin 1:1000 from Sigma, (A2006), Mouse anti-TIM23 1:1000 BD Biosciences (#611222). From Abcam, we used Mouse monoclonal to MTCO1 1:1000 (ab14705), Mouse monoclonal to ATP5A 1:1000 (ab14748), Mouse monoclonal to NDUFA9 1:1000 (ab14713), Mouse monoclonal to SDHA 1:1000 (ab14715), Mouse monoclonal to NDUFB8 1:1000 (ab110242), Mouse monoclonal to UQCRC1 1:2000 (ab110252), Mouse monoclonal to COXIV 1:2000 (ab33985) and Mouse monoclonal to Vinculin 1:5000 (ab18058).

Secondary antibodies: Horseradish Peroxidase-conjugated secondary antibodies were used anti-

mouse 1:5000, anti-rabbit 1:3000, anti-goat 1:5000 (Santa Cruz Biotechnologies), or IRDye 800 conjugated anti–mouse IgG (#610–732–124) and IRDye 700 conjugated anti–rabbit IgG (#610–430–002) (Rockland). Signal was detected by chemiluminiscence using the super Signal West Pico reagent or by scanning using the Odyssey Infrared Imaging System (LI–COR).

BLUE NATIVE POLYACRYLAMIDE GEL ELECTROPHORESIS (BN-PAGE) ANALYSIS

BN-PAGE analysis was performed as described previously (31). Approximately four T-75 flasks were grown at 90% confluency. Cell pellets were collected after trypsin digestion. Membrane dissolution was carried out by addition of 8 mg/mL Digitonin (Sigma), and recovered pellets were resuspended in Aminocaproic Buffer (1.5 M Aminocaproic Acid, 50 mM Bis-Tris) containing protease inhibitors. Approximately 100µg of protein was resuspended in Aminocaproic Buffer and treated with digitonin at a 1:8 ratio (protein:digitonin) (Calbiotech) for 20 minutes. Recovered supernatant was mixed with 0.5% ServaG Dye (5% ServaG (w/v), 0.5 mM EDTA, 50 mM Bis-Tris, 750 mM Aminocaproic Buffer) before loading. 15-30 µg was loaded on a gel. BN-PAGE was carried out in pre-cast 3-12% Bis-Tris Blue Native Gels (Invitrogen, Grand Island, NY). 1X Blue Cathode Buffer (10 mM Tricine, 3 mM Bis-Tris-Cl, pH 7.0, 0.004% (w/v) Serva Blue G Dye) was used to fill the inner chamber and 1X Anode Buffer (50 mM Bis-Tris, pH 7.0) for the outer chamber. Samples were run at 100Vfor 1 hour at 4°C, after which the 1X Blue Cathode Buffer was replaced with 1X Colorless Cathode Buffer (10 mM Tricine, 3 mM Bis-Tris-Cl, pH 7.0) and the gel run at 8 milliamps for 4 hours. Gels were transferred to PVDF membranes overnight at 75V at 4°C. Membranes were dried at 37°C for 15 minutes followed by re-hydration with methanol. Membrane blocking was carried out in 5% milk in PBST for 4 hours before immunoblotting.

ACID-UREA PAGE AND NORTHERN BLOT ANALYSIS

Acid-Urea PAGE and preparation of samples was performed according to (32) with slight modifications. In brief, cells were grown in T150 flask at 90% confluency. Cell pellets were collected after trypsin digestion. Total RNA extraction: The cell pellet was resuspended in Trizol (Invitrogen) and 1/10 volume of sodium acetate Buffer (0.3 M sodium acetate pH 4.5−5.0; 10 mM Na_2EDTA); acid-washed glass beads (0.5 mm diameter; Sigma) were added and RNA was extracted following Invitrogen's instructions for Trizol. The RNA was precipitated with ethanol and recovered by centrifugation at 12,000 *g* for 15 minutes at 4°C, the pellet washed twice with 70% ethanol and finally dissolved in 20−50 µl of 10 mM sodium acetate pH 4.5−5.0 and stored at −80°C until further use. Aminoacyl-tRNAs and formyl aminoacyl-tRNAs were deacylated by base treatment (alkaline treatment) in 0.1 M Tris-HCl pH 9.5 at 65°C for 5 minutes, followed by incubation at 37°C for 1 hour. Aminoacyl-tRNAs were selectively deacylated by treatment with copper sulfate as described (33). Treated RNAs from *Mtfmt* control and *Mtfmt* KO cells were separated by acid-urea PAGE as described previously with modifications (9). Briefly, 0.1 A_{260} units of each RNA sample were loaded onto a 6.5% polyacrylamide gel containing 7 M urea and 0.2 M sodium acetate pH 5.0. The gel was run in the cold room at 500 Volts (~12 V/cm) for approximately 70 hours. Individual tRNAs were detected by Northern blotting using the following hybridization probes: 5'TAGTACGGGAAGGGTATAA3' (mitochondrial $tRNA^{Met}$) and 5'TTCCACTGCACCACTCTGCT3' (cytoplasmic initiator $tRNA_i^{Met}$). Northern blot images were quantified using *Image* Studio™ Lite software (LICOR-Biosciences).

MITOCHONDRIA BIOENERGETICS

Approximately $2x10^5$ cells were seeded in the Seahorse culture plate (3 wells per cell line), and incubated in a 37°C, 5% CO_2 humidified atmosphere for 24 hours. The cell culture medium from the cell plates was replaced the following day with 175 µl/well of pre-warmed low-buffered serum-free Seahorse medium supplemented with Glutamine (2 mM), Sodium Pyruvate (1 mM) and Glucose (10 mM) and incubated at 37°C, in a CO_2-free incubator, for 45 minutes to allow the

temperature and pH of the medium to reach equilibrium before the first rate measurement. The pH of the media was then adjusted to 7.4 with 1 M NaOH. For the mitochondrial respiration rate, the OCR was analyzed in response to oligomycin (1 μM); fluoro-carbonyl cyanide phenylhydrazone (FCCP) (1 μM),; and rotenone plus antimycin A (all Sigma) (1 μM). The measure of Oxigen compsumption rate was used to determined basal respiration, ATP-linked repiration, proton leak, maximum respiratory capacity, spare respiratory capacity and non mitochondrial, . For the glycolysis assay, the ECAR was measured by monitoring changes in pH in intact cells after sequential addition of glucose (10 mM), oligomycin (1 μM) and the inhibitor of the hexokinase 2-DG (2 Deoxy-D-glucose) (75 mM). We measured glycolysis, glycolytic capacity after the addition of oligomycin and estimated the glycolytic reserve as well as the non-glycolytic acidification after the addition of 2-DG. All the calculation were performed accoding to the manufacture parameter guidelines. Measurement of protein concentration was performed at the end of each run to normalize OCR and ECAR by protein content using the Lowry assay (Bio-Rad).

ACTIVITY IN GEL (BN-PAGE)

Approximately 60μg of protein pre-treated with mild digitonin were used for BN-PAGE as described above. For complex I activity the gel was incubated in 0.1 M Tris-HCl (pH 7.4) containing 1 mg/mL of nitrotetrazolum (NTB) and 0.14 mM NADH at room temperature. For complex IV activity, the gel was incubated in 1.54 mM Diaminobenzidine tetrahydrochloride (DAB) dissolved in 50 mM phosphate buffer (pH 7.4). Both reactions were incubated at 37^{o}C for at least 30 minutes and stopped when the brown color for complex IV and blue-purple color for complex I activities appeared.

STATISTICAL ANALYSIS

Statistical significance was analyzed using the Graph Pad software. Two way repeated measures ANOVA analysis of variance followed by Bonferroni post hoc comparison was performed to analyze replicate means and evaluate interaction among the different technical experiments. Two-tail unpaired student t-test was also used to identify statistically significant differences between groups. $P<0.05\%$ was considered significant. Experimental results are shown as mean ± S.D.

Acknowledgements

This work was supported in part by the National Institutes of Health Grants 5R01EY010804, 1R01AG036871 and 1R01NS079965 (C.T.M) and GM17151 (U.L.R). TA was supported by a minority supplement to 5R01EY010804.

Conflict of Interest

The authors declare that they have no conflicts of interest with the contents of this article.

References

1. Christian, B. E., and Spremulli, L. L. (2012) Mechanism of protein biosynthesis in mammalian mitochondria. *Biochim Biophys Acta* **1819**, 1035-1054
2. Kuzmenko, A., Atkinson, G. C., Levitskii, S., Zenkin, N., Tenson, T., Hauryliuk, V., and Kamenski, P. (2014) Mitochondrial translation initiation machinery: conservation and diversification. *Biochimie* **100**, 132-140
3. RajBhandary, U. L. (1994) Initiator transfer RNAs. *J Bacteriol* **176**, 547-552
4. Mai, N., Chrzanowska-Lightowlers, Z. M., and Lightowlers, R. N. (2017) The process of mammalian mitochondrial protein synthesis. *Cell Tissue Res* **367**, 5-20
5. Guillon, J. M., Mechulam, Y., Schmitter, J. M., Blanquet, S., and Fayat, G. (1992) Disruption of the gene for Met-tRNA(fMet) formyltransferase severely impairs growth of Escherichia coli. *J Bacteriol* **174**, 4294-4301
6. Vanunu, M., Lang, Z., and Barkan, D. (2017) The gene fmt, encoding tRNA(fMet)-formyl transferase, is essential for normal growth of M. bovis, but not for viability. *Sci Rep* **7**, 15161
7. Newton, D. T., Creuzenet, C., and Mangroo, D. (1999) Formylation is not essential for initiation of protein synthesis in all eubacteria. *J Biol Chem* **274**, 22143-22146
8. Li, Y., Holmes, W. B., Appling, D. R., and RajBhandary, U. L. (2000) Initiation of protein synthesis in Saccharomyces cerevisiae mitochondria without formylation of the initiator tRNA. *J Bacteriol* **182**, 2886-2892
9. Tucker, E. J., Hershman, S. G., Kohrer, C., Belcher-Timme, C. A., Patel, J., Goldberger, O. A., Christodoulou, J., Silberstein, J. M., McKenzie, M., Ryan, M. T., Compton, A. G., Jaffe, J. D., Carr, S. A., Calvo, S. E., RajBhandary, U. L., Thorburn, D. R., and Mootha, V. K. (2011) Mutations in MTFMT underlie a human disorder of formylation causing impaired mitochondrial translation. *Cell Metab* **14**, 428-434
10. Haack, T. B., Gorza, M., Danhauser, K., Mayr, J. A., Haberberger, B., Wieland, T., Kremer, L., Strecker, V., Graf, E., Memari, Y., Ahting, U., Kopajtich, R., Wortmann, S. B., Rodenburg, R. J., Kotzaeridou, U., Hoffmann, G. F., Sperl, W., Wittig, I., Wilichowski, E., Schottmann, G., Schuelke, M., Plecko, B., Stephani, U., Strom, T. M., Meitinger, T., Prokisch, H., and Freisinger, P. (2014) Phenotypic spectrum of eleven patients and five novel MTFMT mutations identified by exome sequencing and candidate gene screening. *Molecular genetics and metabolism* **111**, 342-352
11. Haack, T. B., Haberberger, B., Frisch, E. M., Wieland, T., Iuso, A., Gorza, M., Strecker, V., Graf, E., Mayr, J. A., Herberg, U., Hennermann, J. B., Klopstock, T., Kuhn, K. A., Ahting, U., Sperl, W., Wilichowski, E., Hoffmann, G. F., Tesarova, M., Hansikova, H., Zeman, J., Plecko, B., Zeviani, M., Wittig, I., Strom, T. M., Schuelke, M., Freisinger, P., Meitinger, T., and Prokisch, H. (2012) Molecular diagnosis in mitochondrial complex I deficiency using exome sequencing. *J Med Genet* **49**, 277-283
12. Neeve, V. C., Pyle, A., Boczonadi, V., Gomez-Duran, A., Griffin, H., Santibanez-Koref, M., Gaiser, U., Bauer, P., Tzschach, A., Chinnery, P. F., and Horvath, R. (2013) Clinical and functional characterisation of the combined respiratory chain defect in two sisters due to autosomal recessive mutations in MTFMT. *Mitochondrion* **13**, 743-748
13. Hinttala, R., Sasarman, F., Nishimura, T., Antonicka, H., Brunel-Guitton, C., Schwartzentruber, J., Fahiminiya, S., Majewski, J., Faubert, D., Ostergaard, E., Smeitink, J. A., and Shoubridge, E. A. (2015) An N-terminal formyl methionine on COX 1 is required for the assembly of cytochrome c oxidase. *Human molecular genetics* **24**, 4103-4113

14. La Piana, R., Weraarpachai, W., Ospina, L. H., Tetreault, M., Majewski, J., Care4Rare Canada, C., Bruce Pike, G., Decarie, J. C., Tampieri, D., Brais, B., and Shoubridge, E. A. (2017) Identification and functional characterization of a novel MTFMT mutation associated with selective vulnerability of the visual pathway and a mild neurological phenotype. *Neurogenetics* **18**, 97-103
15. Oates, A., Brennan, J., Slavotinek, A., Alsadah, A., Chow, D., and Lee, M. M. (2016) Challenges managing end-stage renal disease and kidney transplantation in a child with MTFMT mutation and moyamoya disease. *Pediatr Transplant* **20**, 1000-1003
16. Sinha, A., Kohrer, C., Weber, M. H., Masuda, I., Mootha, V. K., Hou, Y. M., and RajBhandary, U. L. (2014) Biochemical characterization of pathogenic mutations in human mitochondrial methionyl-tRNA formyltransferase. *J Biol Chem* **289**, 32729-32741
17. Arguello, T., and Moraes, C. T. (2015) Cre recombinase activity is inhibited in vivo but not ex vivo by a mutation in the asymmetric spacer region of the distal loxP site. *Genesis* **53**, 695-700
18. Takeuchi, N., Kawakami, M., Omori, A., Ueda, T., Spremulli, L. L., and Watanabe, K. (1998) Mammalian mitochondrial methionyl-tRNA transformylase from bovine liver. Purification, characterization, and gene structure. *J Biol Chem* **273**, 15085-15090
19. Liao, H. X., and Spremulli, L. L. (1991) Initiation of protein synthesis in animal mitochondria. Purification and characterization of translational initiation factor 2. *J Biol Chem* **266**, 20714-20719
20. Spencer, A. C., and Spremulli, L. L. (2004) Interaction of mitochondrial initiation factor 2 with mitochondrial fMet-tRNA. *Nucleic acids research* **32**, 5464-5470
21. Tibbetts, A. S., Oesterlin, L., Chan, S. Y., Kramer, G., Hardesty, B., and Appling, D. R. (2003) Mammalian mitochondrial initiation factor 2 supports yeast mitochondrial translation without formylated initiator tRNA. *J Biol Chem* **278**, 31774-31780
22. Krysko, D. V., Agostinis, P., Krysko, O., Garg, A. D., Bachert, C., Lambrecht, B. N., and Vandenabeele, P. (2011) Emerging role of damage-associated molecular patterns derived from mitochondria in inflammation. *Trends Immunol* **32**, 157-164
23. Rabiet, M. J., Huet, E., and Boulay, F. (2005) Human mitochondria-derived N-formylated peptides are novel agonists equally active on FPR and FPRL1, while Listeria monocytogenes-derived peptides preferentially activate FPR. *Eur J Immunol* **35**, 2486-2495
24. Sasarman, F., and Shoubridge, E. A. (2012) Radioactive labeling of mitochondrial translation products in cultured cells. *Methods Mol Biol* **837**, 207-217
25. Fernandez-Silva, P., Acin-Perez, R., Fernandez-Vizarra, E., Perez-Martos, A., and Enriquez, J. A. (2007) In vivo and in organello analyses of mitochondrial translation. *Methods in cell biology* **80**, 571-588
26. Acin-Perez, R., and Enriquez, J. A. (2014) The function of the respiratory supercomplexes: the plasticity model. *Biochim Biophys Acta* **1837**, 444-450
27. Acin-Perez, R., Bayona-Bafaluy, M. P., Fernandez-Silva, P., Moreno-Loshuertos, R., Perez-Martos, A., Bruno, C., Moraes, C. T., and Enriquez, J. A. (2004) Respiratory complex III is required to maintain complex I in mammalian mitochondria. *Mol Cell* **13**, 805-815
28. Acin-Perez, R., Fernandez-Silva, P., Peleato, M. L., Perez-Martos, A., and Enriquez, J. A. (2008) Respiratory active mitochondrial supercomplexes. *Mol Cell* **32**, 529-539
29. Walker, J. E., Carroll, J., Altman, M. C., and Fearnley, I. M. (2009) Chapter 6 Mass spectrometric characterization of the thirteen subunits of bovine respiratory complexes that are encoded in mitochondrial DNA. *Methods Enzymol* **456**, 111-131

30. Gottlieb, R. A., and Adachi, S. (2000) Nitrogen cavitation for cell disruption to obtain mitochondria from cultured cells. *Methods Enzymol* **322**, 213-221
31. Diaz, F., Barrientos, A., and Fontanesi, F. (2009) Evaluation of the mitochondrial respiratory chain and oxidative phosphorylation system using blue native gel electrophoresis. *Current protocols in human genetics / editorial board, Jonathan L. Haines ... [et al.]* **Chapter 19**, Unit19 14
32. Kohrer, C., and Rajbhandary, U. L. (2008) The many applications of acid urea polyacrylamide gel electrophoresis to studies of tRNAs and aminoacyl-tRNA synthetases. *Methods* **44**, 129-138
33. Schofield, P., and Zamecnik, P. C. (1968) Cupric ion catalysis in hydrolysis of aminoacyl-tRNA. *Biochim Biophys Acta* **155**, 410-416

Figure Legends

Figure 1. *Mtfmt* homozygous knockout fibroblasts do not express MTFMT protein (A) Generation of the *Mtfmt* KO mouse skin derived fibroblast model using the cre-loxP technology. Exon 4 flanked by loxP sites (5'loxP and 3'loxP, grey triangles) in a parental clone (loxP/loxP) was removed by transfection with a plasmid expressing cre recombinase (cre) and confirmed by PCR amplification using specific primers (black arrows). Positive clones (+) deleted exon 4 results in a putative fragment of 609 bp and no retention of 5' (539 bp) and 3' loxP (274 bp) amplicons. (B) Western blot of crude mitochondria enriched fractions. *Mtfmt* KO cells (n=3) showed absence of MTFMT. TIM23 was used as mitochondria loading control, and NIH3T3 mouse fibroblast cells as a positive control of MTFMT expression.

Figure 2. Mitochondrial MTFMT is responsible for N-formylation of the Met-tRNA^{Met} in mammalian mitochondria. (A) Analysis of tRNAs by acid urea polyacrylamide gel electrophoresis allows the separation of the three forms of tRNA^{Met} in RNA extracted under acidic conditions (sodium acetate). Treatment with copper sulfate deacylates only Met-tRNA^{Met} allowing the visualization of fMet-tRNA^{Met}. Alkaline treatment deacylates both fMet-tRNA^{Met} and Met-tRNA^{Met} allowing the visualization of the total levels of tRNA^{Met}. Absence of N-formylation in *Mtfmt* KO clones compared to control cell clones and preferential accumulation of the Met-tRNA^{Met} is shown in the upper panel. Cytoplasmic initiator methionine tRNA (tRNA$_i^{-Met}$) was used as internal control (bottom panel). (B) Quantification of the three forms of tRNA^{Met}, expressed as a percent of control and presented as mean±SD. unpaired two way ANOVA was used for statistics *P<0.05. (n=3). (C) Quantification of total mitochondrial tRNA^{Met} in *Mtfmt* KO clones, expressed as ratio of mitochondrial tRNA^{Met} over cytoplasmic initiator tRNA$_i^{Met}$, with *Mtfmt* control samples set to 100% (*P<0.0256)

Figure 3. Mitochondrial protein synthesis in *Mtfmt* KO fibroblast clones occurs in the absence of N-formylation. (A) Representative pattern of a ^{35}S-Met-Cys pulse-labeled mitochondrial translation (30 minutes) in the presence of emetine as a cytoplasmic protein synthesis inhibitor. Fast green staining was used as a total loading protein control, β actin as a cytoplasmic and TIM23 as mitochondrial control. (B) Absence of N-formylation in the *Mtfmt* KO cells resulted in faster migration of the ND1 (black arrow head). (C) Individual rates of mitochondrial protein synthesis of *Mtfmt* KO cells (red) expressed as percent of control (black) and normalized to fast green staining. Data from 3 independent short pulse experiments (3 clones each)) are presented as mean±S.D. Two way ANOVA with Bonferroni correction was used to compare each subunit. *P<0.05, **P<0.01. (BD) Below Detection, (n.s) no significant. COII and ATP6 have the same expected size and were quantified as one band.

Figure 4. Absence of N-formylation does not affect the stability of newly synthesized subunits in the first 18 hours. The rate of degradation of each polypeptide in the *Mtfmt* KO cells was measured as percent of decay from ^{35}S-Met-Cys incorporation at 30 minutes (pulse- 0.5 hr) in the presence of anisomycin (a reversible cytosolic protein synthesis inhibitor) followed by chase at 9 and 18 hours. There were no major changes in the stability of the mitochondrially synthesized polypeptides. ATP8 levels were increased at 9 hours in controls (p<0.01). Results are expressed as mean±S.D of 3 different cell clones (CTR in black, KO in red); . Ponceau and fast green staining were used as loading controls and two-way ANOVA was used for analyses. ND3 was not detected at 18 hours

and COII and ATP6 have the same expected size and were quantified as one band.

Figure 5. Absence of N-formylation affects the steady-state levels of OXPHOS complexes. (A) Representative western blots from total protein lysates show decrease levels of NDUFB8 subunit (** P<0.007) of complex I and COIV (** P<0.006) of complex IV in *Mtfmt* KO cells. No significant changes were observed in other OXPHOS markers. (B) Values are expressed as a percent of control (CTR) and represent mean±S.D of 3 independent experiments (3 clones each) for NDUFB8, NDUFA9 and COI or 3 clones for the other markers. Vinculin (VINC) and Tubulin (TUB) were used as loading controls. VINC blots were the same for: (CIV and SDHA); (NDUFA9 and NDUFB8); (TIM23 and ATP5A); (UQCRC1). TUB was the loading control for (COI). Two tail t-test was used for statistical analyses.

Figure 6. Absence of N-formylation affects assembly of complex I and IV and supercomplexes. (A) Analysis of OXPHOS complex and supercomplex assembly was done by blue native gels (BN-PAGE) in the presence of digitonin followed by western analyses and using the antibodies in parenthesis to identify each complex. Note the near absent CI-III_2-CIV_n supercomplex and decreases in complexes I and IV. All values were normalized to TIM23. (B) Data are presented as mean±S.D of 3 clones and unpaired two way ANOVA was used for statistics (*P<0.05. **P<0.01 ***P<0.001). Total levels of complex I, II, III, IV and Vwere analyzed using unpaired two tailed student t-test. (C) BN-PAGE in gel activity showed decreased activity of free complex I (CI) and supercomplexes (CI-III_2 and CI-III_2-CIV_n) in *Mtfmt* KO cells and decreased free complex IV (CIV) activity. TIM23 was used as a loading control.

Figure 7. Absence of N-formylation results in increase of glycolysis rate in *Mtfmt* KO cells. (A) Mitochondria respiration rate of *Mtfmt* KO intact cells measured using the oxygen consumption rate (OCR) and expressed in percent of control showed decrease basal respiration (*P<0.0469), mitochondrial proton-leak respiration (*P<0.022), (calculated as the OCR difference after the addition oligomycin and rotenone/antimycin) and increased spare respiratory capacity (***P<0.0005, measured as the difference between maximal respiration -OCR after addition of FCCP- and basal respiration) (B) Measurements of glycolytic function in *Mtfmt* KO cells using the extracellular acidification rate (ECAR) showed increased basal glycolysis (**P<0.005) and decreased glycolytic reserve (*P<0.022, calculated as the difference between the basal glycolysis after adding glucose and the glycolytic capacity after addition of oligomycin). Data are presented as mean±S.D analyzed using unpaired two tailed student t-test. n=6 independent experiments for OCR or n=5 (CTR),n=4 (KO) for ECAR (3 technical replicates each) respectively.

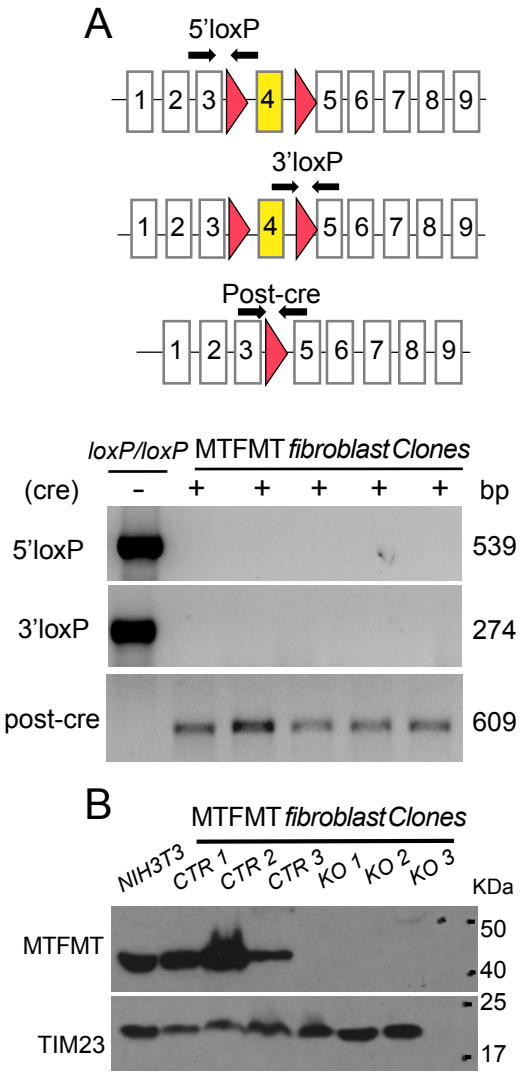

Figure 1

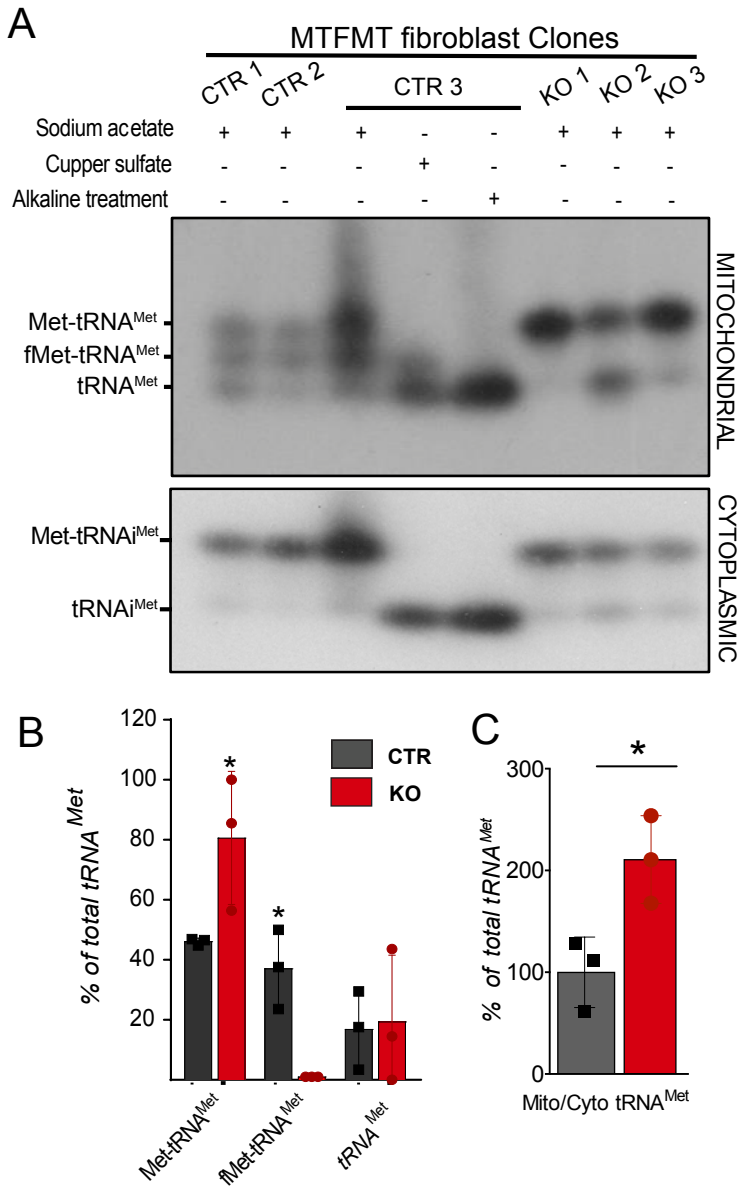

Figure 2

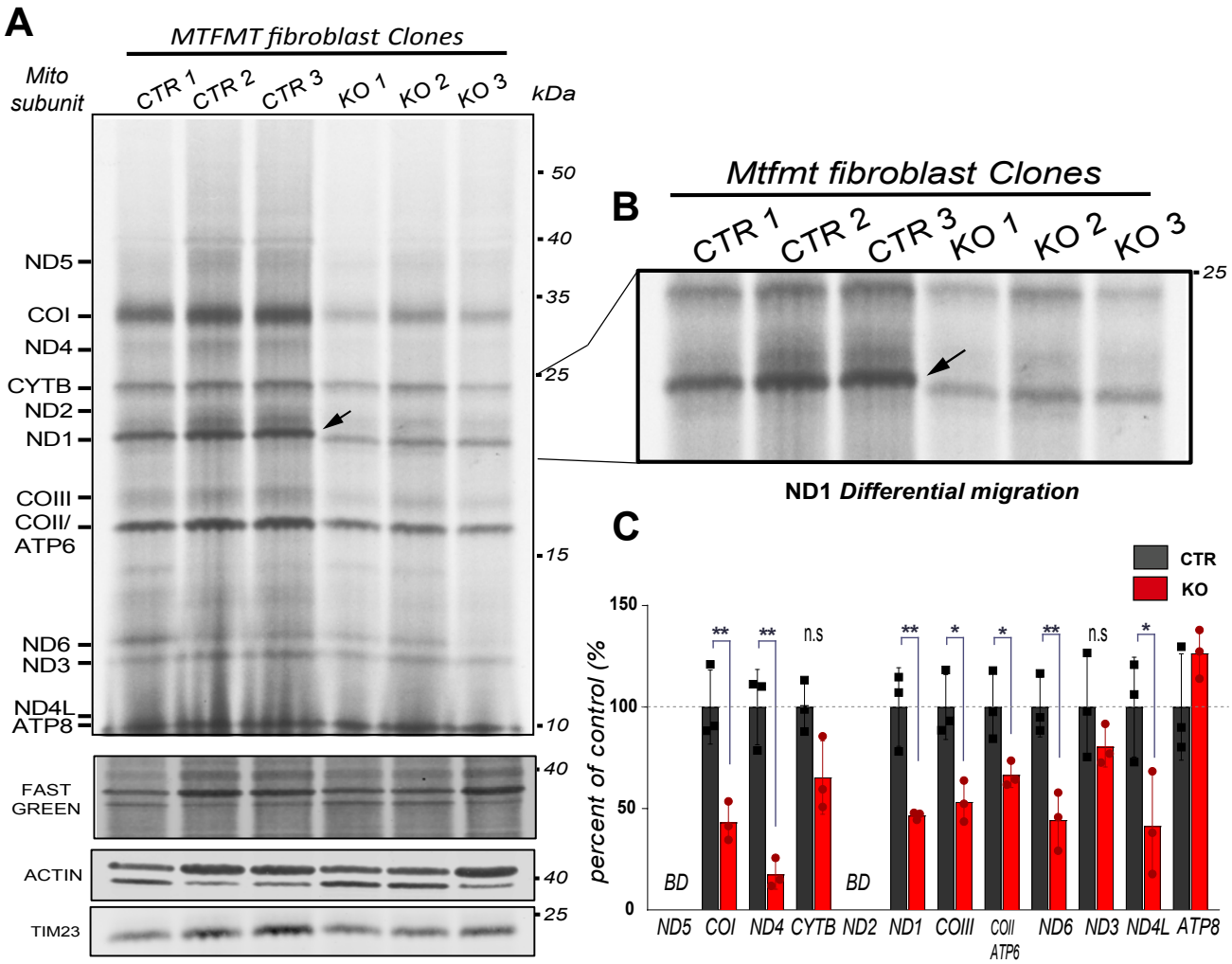

Figure 3

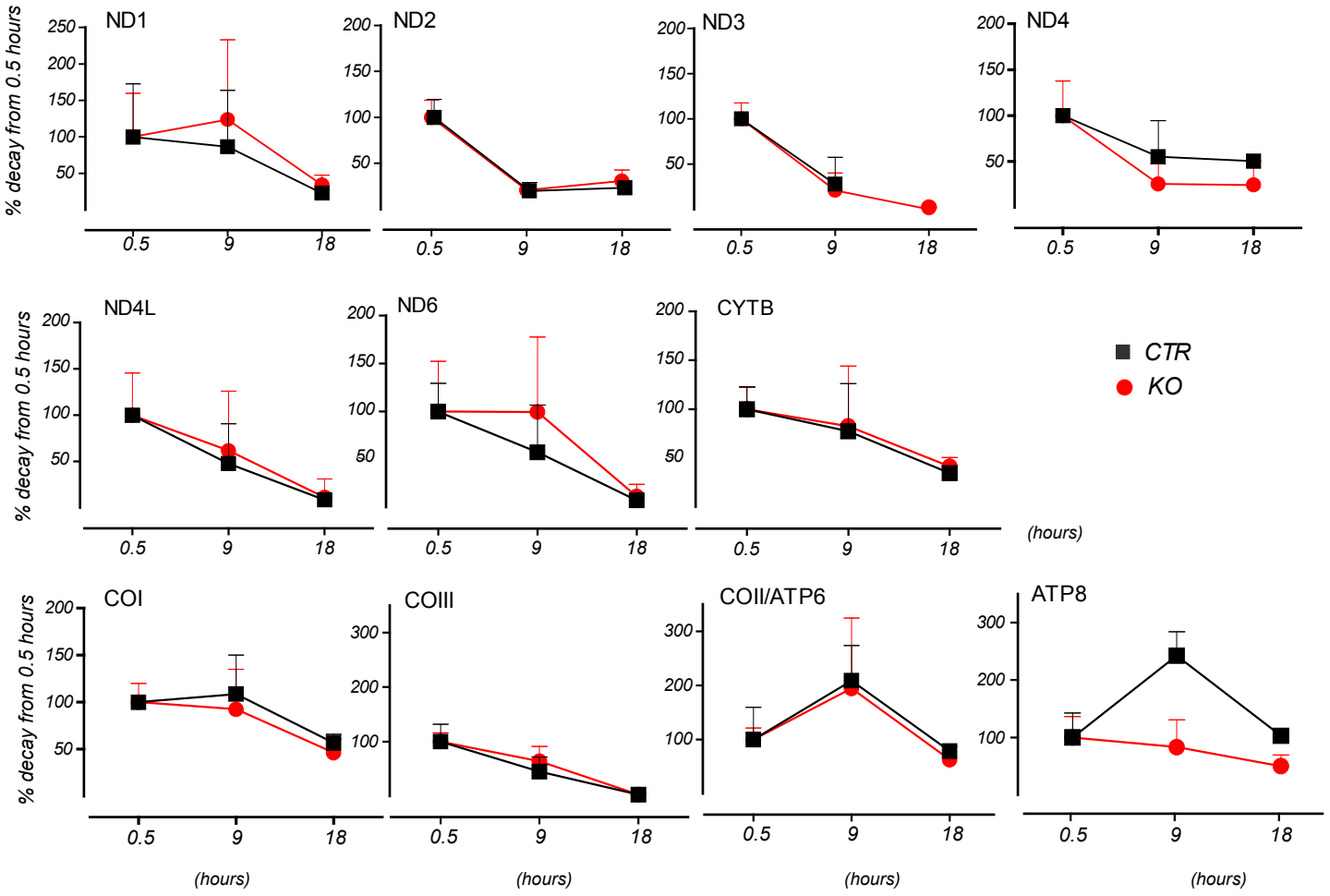

Figure 4

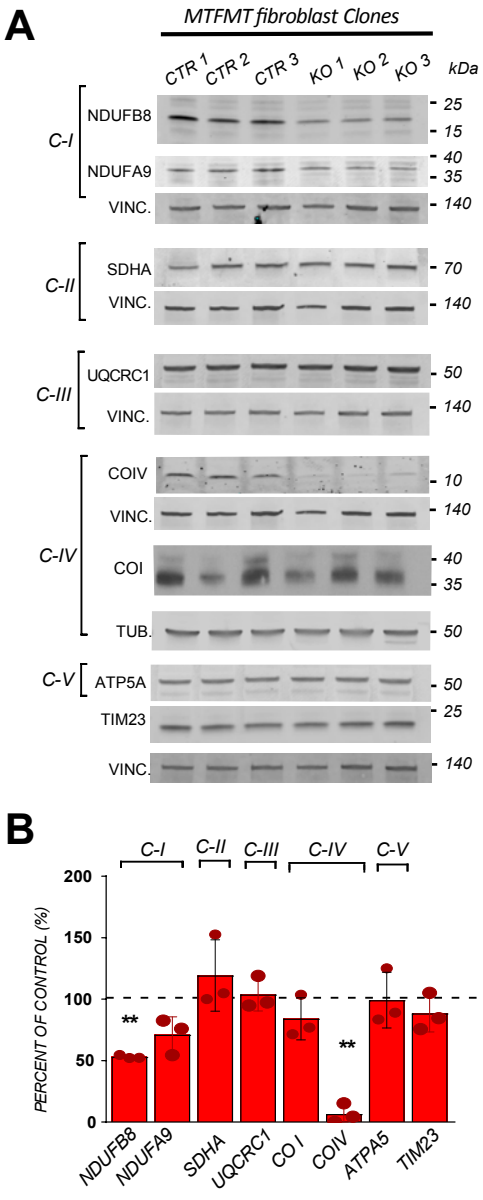

Figure 5

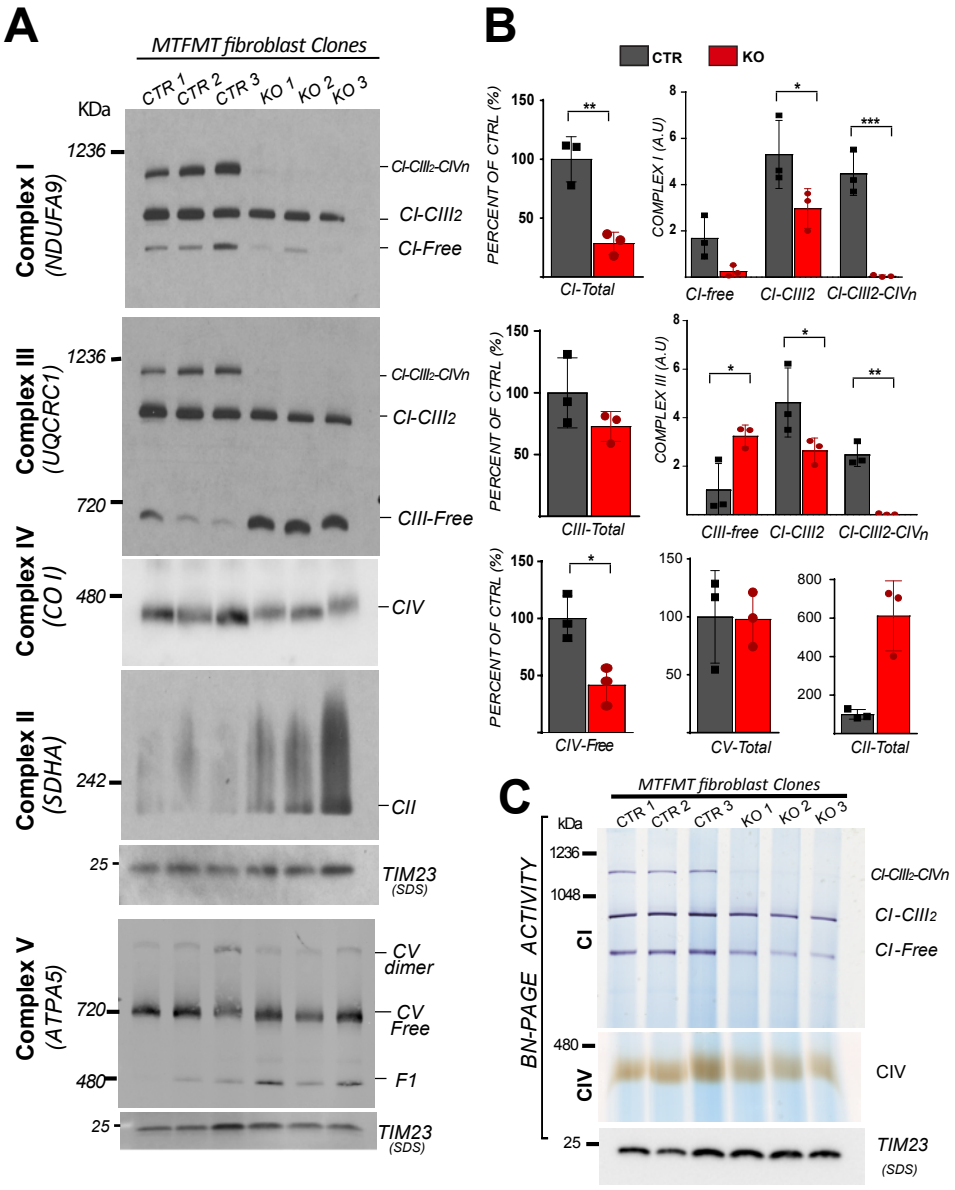

Figure 6

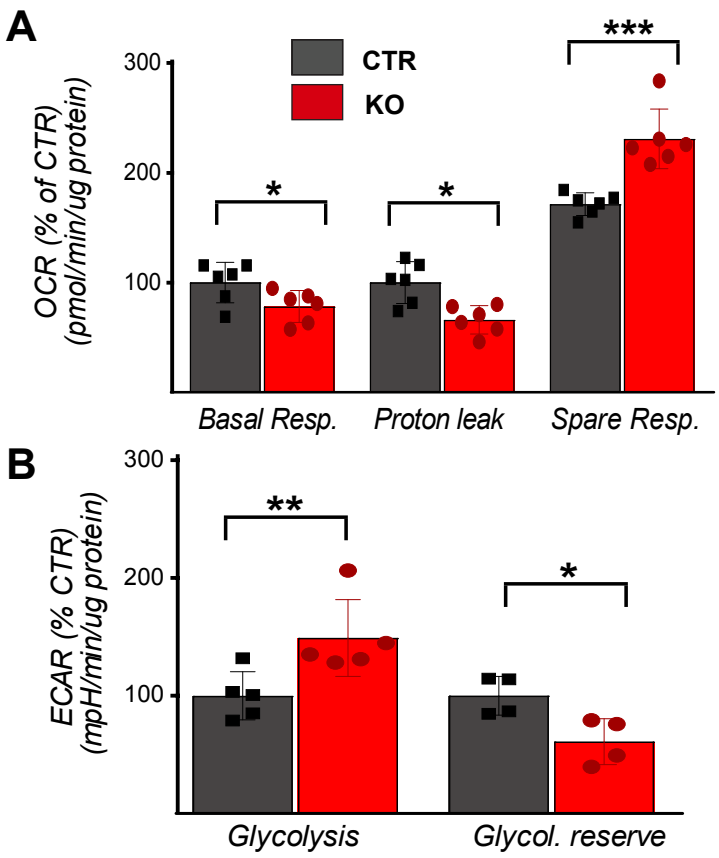

Figure 7

Mitochondrial methionyl N-formylation affects oxidative phosphorylation complexes steady-state levels and their organization into supercomplexes

Tania Arguello, Caroline Köhrer, Uttham L. RajBhandary and Carlos T. Moraes

J. Biol. Chem. published online August 7, 2018